ScienSage

Journal of Advanced Scientific Research

Available online through http://www.sciensage.info

ISSN
0976-9595
Research Article

COUMARIN-DIHYDROPYRIMIDINONE HYBRIDS: DESIGN, VIRTUAL SCREENING, SYNTHESIS AND CYTOTOXIC ACTIVITY AGAINST BREAST CANCER

Rohit Bhatia*[1, 2], Raj K. Narang[3], Ravindra K. Rawal[4]

[1]*Research Scholar, Department of Pharmaceutical Sciences & Technology, MRSPTU, Bathinda, Punjab, India*
[2]*Department of Pharmaceutical Chemistry, ISF College of Pharmacy, Ferozepur G.T. Road, Moga, Punjab, India*
[3]*Department of Pharmaceutics, ISF College of Pharmacy, Ferozepur G.T. Road, Moga, Punjab, India*
[4]*Department of Chemistry, Maharishi Markandeshwar (Deemed to be University), Mullana, Haryana, India*
**Corresponding author: bhatiarohit5678@gmail.com*

ABSTRACT

Breast cancer is the most invasive form of cancer in women. It is characterized by over production of oestrogens which is mainly mediated by over-expression of aromatase. In the presented work we have designed a library of fifty coumarin-dihydropyrimidinone hybrids and screened them virtually for their aromatase inhibitory potentials through molecular docking tools. Docking was carried out against human aromatase (PDB Id: 3S7S) using exemestane as standard drug. Six compounds with best docking scores and interactions were selected and also analysed for *in silico* drug likeliness and toxicity. Further these six compounds were synthesized and characterized through spectrometric techniques. Further these were evaluated for cytotoxic potentials against breast cancer cell lines using MTT assay. Compounds **CD8** and **CD28** were found most potent among the all. The synthesized compounds must be explored further for discovery of a suitable therapeutic candidate against breast cancer.

Keywords: Breast cancer, Aromatase, Coumarin, Dihydropyrimidinone, Hybrids, MOE

1. INTRODUCTION

Despite of a great advancement in health and medical service sector, cancer is still a major life threatening disease around the globe [1-4]. Breast cancer is one of the most lethal forms of cancer in women and leading cause of death in post menopausal women. It has been reported that almost 66% of post menopausal breast cancer occurs due to over expression of oestrogen which leads to emergence of hormone-dependent tumors [5]. Oestrogen binds to its receptors present in mammary cells and is responsible for development of tumors in female breasts [6]. Aromatase belongs to cytochrome P450 enzyme class which is present in ovaries of premenopausal, adipose tissue of postmenopausal and placenta of pregnant women in higher concentrations [7]. It is evident that aromatase is highly expressed in tumor sites of breasts [8, 9]. Therefore aromatase has been identified as a significant target for development of therapeutic agents against breast cancer. There is a huge number of medicines/chemotherapeutic agents working through different targets/modes, already available in market against breast cancer and other cancers. Beyond this, there is still selectivity and normal cell toxicity issues are there which are limiting the use of existing therapeutic agents [10]. Many scientists, researchers, academicians and industries from all over the world are working continuously towards developing therapeutic candidates against cancer with least toxicity and high selectivity. Pathophysiology and progression of breast cancer involves a series of complex underlying events and many of the single targeted agents fail to achieve the therapeutic action. Therefore either high dose or a combination of multiple drugs is required to treat the ailment which generally leads to toxicity [11]. To combat this issue researchers and medicinal chemists have focussed their attention towards concept of molecular hybridization. This approach is based upon generation of new hybrid molecule by combining two or more scaffolds/sub unit of scaffold having different mode of actions [12] through suitable chemical approach. The hybrid molecule thus created possesses all the therapeutic potentials of individual moieties and is able to bind to more than one therapeutic target [13, 14]. Hence this is an ideal approach to design multi-target directed therapeutic agents against cancer.

Coumarin scaffold is one of the well established motifs, which has displayed promising anticancer potentials by interacting through various biological targets. Coumarin possesses various sites which can be explored for development of therapeutic agents against breast cancer. There are several reported coumarin hybrids which have displayed excellent activity against breast cancer as well as other forms of cancer [15-20]. Beyond this coumarin derivatives have reported very rare extent of organ toxicity which makes it ideal to be selected for development of anticancer agents. It is evident that coumarin derivatives have tendency to interact with aromatase, sulphatase, protein kinase, selective estrogen receptor modulator, human epidermal growth factor receptor etc. [12]. Dihydropyrimidinone (DHPM) is another moiety which has been continuously explored for its anti-cancer acclivity. Also, this class of compounds causes mitotic arrest at G2/M phase by blocking bipolar mitotic spindle in mammalian cells leading to cell apoptosis. There are several reports has been available in literature which give success story of dihydropyrimidinone derivatives as cytotoxic agents [21-25].

So with intent to discover new therapeutic candidates against breast cancer, we designed a library of 50 coumarin-dihydropyrimidinone hybrids so as to get the therapeutic efficacy of both the scaffolds in single molecule. Molecular docking is a significant approach to predict the binding patterns of designed molecules with the target. Therefore, we virtually screened out the compounds with best binding scores and binding patterns with aromatase through molecular docking tools. We screened out six best compounds out of fifty and synthesized them with the help of suitable synthetic protocol. The synthesized compounds were further characterized and evaluated for cytotoxic activity against breast cancer cell lines. The compounds were also subjected to *in silico* drug likeliness and toxicity prediction studies. The rationale behind the designed compounds has been outlined in **Fig. 1.**

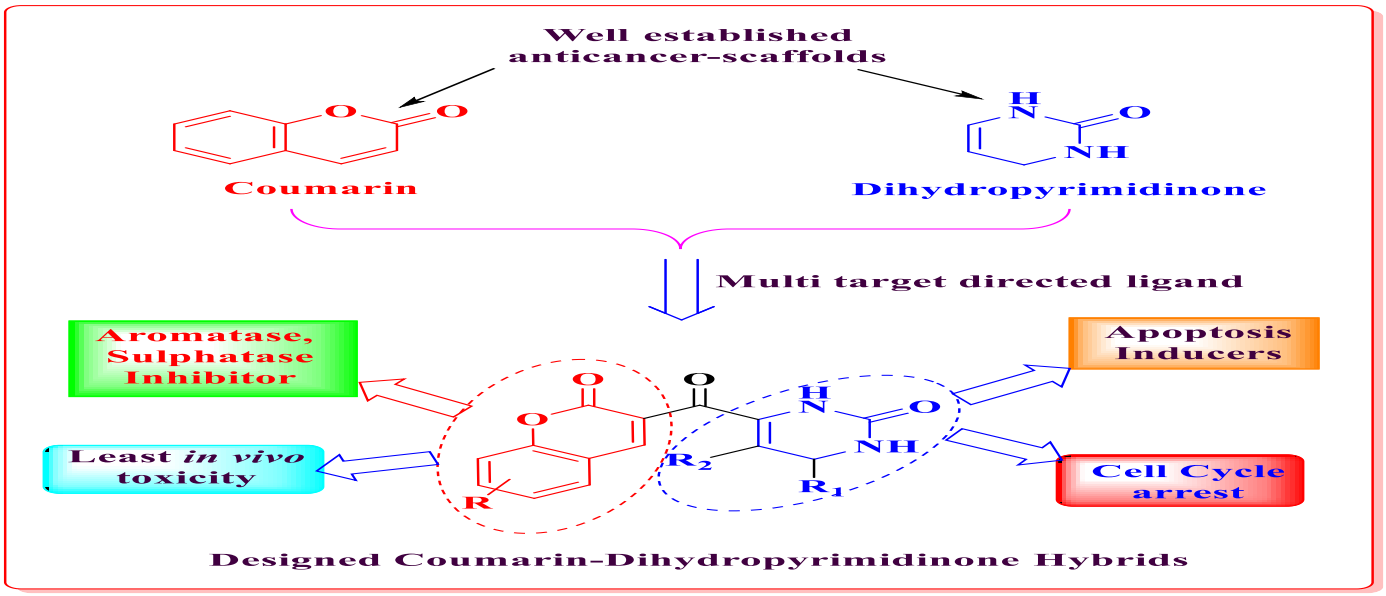

Fig. 1: Design strategy for Coumarin-Dihydropyrimidinone Hybrids

2. EXPERIMENTAL

2.1. Molecular Docking

A library of fifty coumarin-dihydropyrimidinone hybrids was generated by substituting various positions with different substituents. The designed library of molecules was subjected to molecular docking studies against human aromatase (PDB Id: 3S7S) using MOE software version 2019.0102 (license provided by chemical computing group). The 3D crystal structure of human aromatase (PDB Id: 3S7S) were procured from RCSB-PDB (http:/www.rcsb.org/pdb) in pdb format [26]. The protein pocket was prepared by addition of hydrogens, deleting the internal ligands, deletion of waters/cofactors followed by isolation of atoms. 3D structures of prepared aromatase cavity have been depicted in Fig. 2. The 2D structures of all the designed molecules were drawn in Chem Biodraw 15.0 software and were saved as mol files. The 2D structures were

energy minimized by selecting MMFF94x forcefield, with gradient value of 0.0001 kcal/mol. The energy minimized ligands were saved as tripos mol2 files and converted into mdb.mol files in the MOE wizard.

The prepared mdb.mol files of the molecules were further subjected to molecular docking in the prepared cavity of human aromatase. Various selections were made using the compute wizard and various steps like selection of protein, upload of mdb.mol files, selection of site and run were followed. Among the fifty compounds, top six compounds with maximum scores were selected and further analysed for studying the binding patterns with the help of 2D and 3D poses in JPEG format. The orientation poses were then compared with the standard aromatase inhibitor drug. The docking protocol was validated by re-docking the internal ligand and reproducing its confirmation. Root mean square deviation was calculated as a validation parameter.

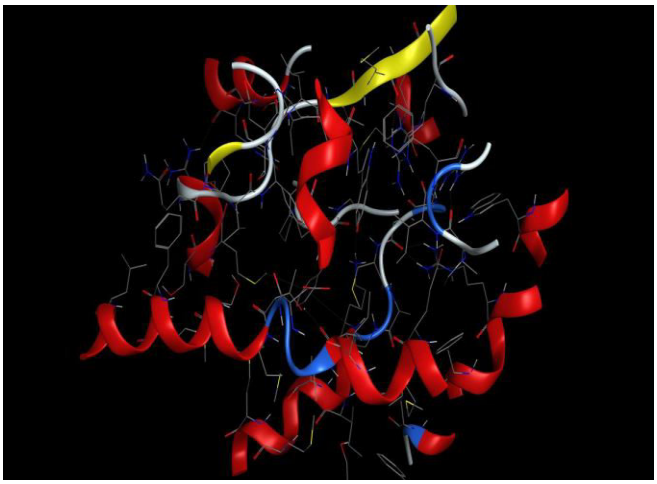

Fig. 2: Cavity of Human aromatase (PDB Id: 3S7S)

2.2. *In silico* drug likeliness prediction

The best 6 compounds discovered by molecular docking studies were further evaluated for their drug like properties. The predictions were made on the basis of Lipinski's rule of five which states that for a molecule to behave as a drug it must have: number of hydrogen bond donors less than 5; number of hydrogen bond acceptors should not be more than 10; molecular mass should be less than 500 daltons; number of rotatable bonds should not be less than 10 and log P (octanol-water partition coefficient) should not be greater than 5. The predictions were made using Swiss ADME online tool [27].

2.3. *In silico* toxicity prediction

In silico toxicity prediction studies are significant to get an idea about the toxicity of the molecules on normal cells and tissues. These predictions also provide an idea about the toxic dose for different compounds. These studies are economic, less time consuming without use of any experimental animal. In the present study, the toxicity of best 6 compounds was estimated using PreADME and Potox-II online web tool. PreADME estimates toxicity on animals and human ether related gene (associated with cardiotoxicity) whereas Protox calculates the lethal dose as well as the toxicity class [28].

2.4. Synthesis

2.4.1. Chemicals and Reagents

Various chemicals, reagents and solvents were purchased in purified form from different chemical agencies including Sigma-Aldrich, Merck and Lobachemie. Melting points were determined using COMPLAB capillary melting point apparatus and were uncorrected. The progress of the reactions was monitored by thin layer chromatography utilizing precoated aluminium plates and UV-chamber and iodine were used as visualising agents. ^{1}H NMR and ^{13}C NMR spectra were recorded on a Bruker AM 300 (300 MHz) or a Bruker Avance III 500 (500 MHz; 13C NMR at 75 and 125 MHz) spectrometer (Bruker Biosciences) using $CDCl_3$ or DMSO as solvent. Chemical shifts (δ) were expressed as parts per million (ppm), using tetramethylsilane as the internal standard and splitting were expressed as singlet (s), doublet (d) and multiplet (m). Mass spectra were taken in ESI mode on an Agilent 1100 LC-MS.

2.4.2. Synthetic procedures and characterization data of synthesized compounds

2.4.2.1. Synthesis of substituted 3-acetoacetyl coumarins 4 (1-(2-oxo-2H- chromen-3-yl)butane-1,3-dione)

Eight (8) ml (0.07mol) of substituted salicyaldehyde **1** was mixed with 9.2ml (0.07 mol) of ethylacetoacetate **2**; the mixture was basified with piperidine and stirred under cold conditions for 2 hours. The mixture was neutralized by addition of 1M HCl solution to obtain compound substituted 3-acetyl coumarins **3**. Compound **3** (7.52g, 0.04 mol) was further dissolved in ethyl acetate (15 ml) and stirred under cold conditions. Further solution of potassium tertiary butoxide (2.24 g, 0.04 mol) in toluene was introduced dropwise to the mixture with continuous stirring. After two hours

potassium salt of 3-acetoacetyl coumarin separates out and the mixture was kept in ice box overnight. The solid was filtered by aid of ether, dissolved in cold water and acidified with acetic acid. The crude 3-acetoacetyl coumarin **4** was again filtered, air dried and recrystallized from ethanol.

2.4.2.2. Synthesis of substituted 6-methyl-5-(2-oxo-2H-chromene-3-carbonyl)-4-phenyl-3,4-dihydropy rimidin-2(1H)-ones

Approximate 1.8 g (0.007 mol) of compound 4 was mixed with 2.8 ml of substituted benzaldehydes 5 and 1.2 g of urea and refluxed in the presence of acetonitrile and sulphuric acid for 4 hours. The oily liquid was then poured in water and target compounds CD (6, 8, 19, 20, 28, 44) were precipitated out as solid mass. It was filtered, washed with cold water and recrystallized from ethanol.

2.4.3. Characterization of Synthesized compounds

2.4.3.1. Compound 4 (3-acetoacetyl coumarin)

^{1}H NMR (300 MHz, $CDCl_3$) δ 2.32(s, 3H, OCH_3); 4.18 (s, 2H, CH_2); 7.45-7.49 (m, 2H, Ar-CH); 7.52 (t, 1H, Ar-CH); 7.72 (d, 1H, Ar-CH); 8.52 (s, 1H, pyrone-CH).

2.4.3.2. Compound CD6 (4-(4-hydroxyphenyl)-5-(7-methoxy-2-oxo-2H-chromene-3-carbonyl)-6-methyl-3,4-dihydropyrimidin-2(1H)-one)

^{1}H NMR (300 MHz, $CDCl_3$) δ 2.32(s, 3H, CH_3); 3.78 (s, 3H, OCH_3); 5.18 (s, 1H, CH); 6.68(d, 2H, Ar-CH); 6.95-6.97 (m, 4H, Ar-CH); 7.52 (s, 1H, NH); 7.62 (d, 1H, Ar-CH); 8.52 (s, 1H, pyrone-CH); 9.04-9.08 (d, 2H, OH & NH). ^{13}C NMR (500 MHz, $CDCl_3$) δ 17.8, 51.2, 55.6, 100.5, 110.4, 115.4, 118.3, 126.1, 126.2, 129.8, 134.4, 135.8, 147.6, 150.2, 154.2, 154.8, 156.6, 159.7, 160.4, 199.2. HRMS (micro TOF-QII, MS, ESI): m/z $[M+H]^+$ Calculated for $C_{22}H_{18}N_2O_6$ 406.39, Obsd. 406.12.

2.4.3.3. Compound CD8 (5-(7-methoxy-2-oxo-2H-chromene-3-carbonyl)-4-(4-methoxyphenyl)-6-methyl-3,4-dihydropyrimidin-2(1H)-one)

^{1}H NMR (300 MHz, $CDCl_3$) δ 2.28(s, 3H, CH_3); 3.81-3.84 (d, 6H, OCH_3); 5.18 (s, 1H, CH); 6.68(d, 2H, Ar-CH); 7.01-7.16 (m, 4H, Ar-CH); 7.52 (s, 1H, NH); 7.62 (d, 1H, Ar-CH); 8.52 (s, 1H, pyrone-CH); 9.08 (s, 1H, NH). ^{13}C NMR (500 MHz, $CDCl_3$) δ 17.7, 51.2, 55.8, 55.8 100.5, 110.1, 115.7, 118.2, 125.1, 125.2, 129.8, 135.4, 135.8, 147.9, 151.2, 154.2, 154.8, 156.6, 159.3, 161.4, 199.2. HRMS (micro TOF-QII, MS, ESI): m/z $[M+H]^+$ Calculated for $C_{23}H_{20}N_2O_6$ 420.47, Obsd. 420.12.

2.4.3.4. Compound CD19 (5-(7-chloro-2-oxo-2H-chromene-3-carbonyl)-4-(4-chlorophenyl)-6-methyl-3,4-dihydropyrimidin-2(1H)-one)

^{1}H NMR (300 MHz, $CDCl_3$) δ 2.28(s, 3H, CH_3); 5.13 (s, 1H, CH); 7.18-7.31 (m, 6H, Ar-CH); 7.51 (s, 1H, NH); 7.72 (d, 1H, Ar-CH); 8.59 (s, 1H, pyrone-CH); 9.04 (s, 1H, NH). ^{13}C NMR (500 MHz, $CDCl_3$) δ 17.7, 51.2, 116.5, 118.1, 119.7, 125.2, 126.1, 126.2, 128.8, 128.8, 132.6, 134.7, 135.4, 141.8, 147.9, 150.2, 154.2, 154.8, 159.3, 199.2. HRMS (micro TOF-QII, MS, ESI): m/z $[M+H]^+$ Calculated for $C_{21}H_{14}Cl_2N_2O_4$ 429.17 Obsd. 428.82.

2.4.3.5. Compound CD20 (5-(7-chloro-2-oxo-2H-chromene-3-carbonyl)-4-(4-fluorophenyl)-6-methyl-3,4-dihydropyrimidin-2(1H)-one)

^{1}H NMR (300 MHz, $CDCl_3$) δ 2.28(s, 3H, CH_3); 5.13 (s, 1H, CH); 7.21-7.39 (m, 6H, Ar-CH); 7.51 (s, 1H, NH); 7.62 (d, 1H, Ar-CH); 8.56 (s, 1H, pyrone-CH); 9.09 (d, 1H, NH). ^{13}C NMR (500 MHz, $CDCl_3$) δ 17.7, 51.2, 115.5, 115.7, 116.7, 118.2, 119.1, 125.2, 128.8, 128.8, 129.6, 134.7, 135.4, 138.8, 147.9, 150.2, 154.4, 154.8, 160.2, 199.2. HRMS (micro TOF-QII, MS, ESI): m/z $[M+H]^+$ Calculated for $C_{21}H_{14}ClFN_2O_4$ 412.87 Obsd. 412.12.

2.4.3.6. Compound CD28 (6-methyl-5-(7-nitro-2-oxo-2H-chromene-3-carbonyl)-4-(p-tolyl)3,4-dihydropy rimidin-2(1H)-one)

^{1}H NMR (300 MHz, $CDCl_3$) δ 2.12-2.28 (d, 6H, CH_3); 5.13 (s, 1H, CH); 7.09 (d, 2H, Ar-CH); 7.29 (d, 2H, Ar-CH); 8.21-8.29 (m, 3H, Ar-CH); 7.51 (s, 1H, NH); 8.56 (s, 1H, pyrone-CH); 9.09 (s, 1H, NH). ^{13}C NMR (500 MHz, $CDCl_3$) δ 17.7, 21.4, 51.2, 112.5, 118.7, 120.7, 124.2, 126.1, 126.2, 128.4, 128.4, 129.8, 134.8, 136.6, 140.7, 141.2, 141.2, 150.4, 154.8, 159.2, 199.2. HRMS (micro TOF-QII, MS, ESI): m/z $[M+H]^+$ Calculated for $C_{22}H_{17}N_3O_6$ 419.47 Obsd. 419.07.

2.4.3.7. Compound CD44 (4-(4-aminophenyl)-6-methyl-5-(7-methyl-2-oxo-2H-chromene-3-carbonyl)-3,4-dihydropyrimidin-2(1H)-one)

^{1}H NMR (300 MHz, $CDCl_3$) δ 2.22-2.24 (d, 6H, CH_3); 4.91 (s, 2H, NH_2); 5.13 (s, 1H, CH); 6.49 (d, 2H, Ar-

CH); 6.69 (d, 2H, Ar-CH); 7.11-7.19 (d, 2H, Ar-CH); 7.51 (s, 1H, NH); 7.78 (d, 1H, Ar-CH); 8.51 (s, 1H, pyrone-CH); 9.09 (s, 1H, NH). ^{13}C NMR (500 MHz, $CDCl_3$) δ 17.7, 21.3, 51.2, 115.02, 115.02, 115.1, 117.5, 118.7, 125.7, 126.1, 126.2, 128.4, 133.4, 134.8, 143.6, 146.7, 147.2, 150.2, 154.4, 154.8, 159.2, 199.2. HRMS (micro TOF-QII, MS, ESI): m/z $[M+H]^+$ Calculated for $C_{22}H_{19}N_3O_4$ 3899.47 Obsd. 389.11.

2.5. Cytotoxic Activity

The cytotoxic activity of the synthesized compounds was evaluated through colorimetric MTT (3-(4,5-dimethylthiazol-2-yl)-2,5-diphenyl-2H-tetrazolium bromide) assay. This assay is based upon the potential of NADPH dependent cellular oxidoreductases to reduce the tetrazolium dye MTT to convert it into insoluble purple colored form formazan. The anti-breast cancer activity of the synthesized coumarin-dihydropyrimi - dinone derivatives was evaluated against breast cancer cell lines MCF7 and T47D utilizing MTT assay protocol [29]. Exemestane was used as reference drug for comparison of results. Cell cytotoxicity was determined by extent of MTT reduction by cells when treated with synthesized compounds. The precultured cells were loaded on a 96-well plate at a concentration of 10000 cells per well and allowed to stick on for 24 hours. Each treatment of compound consisted of five replicates and allowed to culture for 48 to 72 hours. 20µL of MTT (5 mg/mL) was added to each well and culturing was done for 4 hours. After proper culturing the supernatant was romed and 150 µL of DMSO was added to each well followed by incubation at 37°C for 30 min and then swirled for 10 min. The absorbance at 570 nm was measured using a microplate reader. Each determination was repeated three times. The graphs and statistical analysis was carried out using GraphPad Prism 7 software.

3. RESULTS AND DISCUSSION

3.1. Binding patterns of designed molecules with aromatase

The designed compounds (CD1-CD50) were subjected to molecular docking against human aromatase (PDB Id: 3S7S) using MOE software. Maximum compounds get fit inside the pocket of aromatase. Various docking scores displayed by the designed compounds have been displayed in **Table 1.** The docking protocol validated and RMSD value was found to be 1.12. The docking results were compared with marketed well established aromatase inhibitor drug exemestane. Among fifty designed molecules, six displayed excellent docking scores among the whole library of compounds. These six were estimated to possess maximum aromatase inhibitory potentials among all designed molecules. These best six compounds were further analysed with the help of 2D and 3D binding poses to study the fitting capability inside the receptor, type of interactions involved with the receptor and distance of interactions between compounds and receptor.

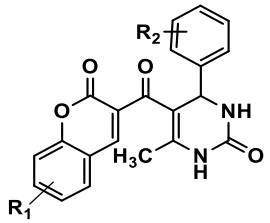

Designed Compounds (CD1-CD50)

Table 1: Docking Scores of Designed Library of Compounds

Compound	R_1	R_2	Docking Scores (PDB Id: 3S7S)
CD1	H	H	-9.18
CD2	H	4-OH	-9.32
CD3	H	4-CH_3	-8.68
CD4	H	4-OCH_3	-8.23
CD5	H	4-Cl	-8.62
CD6	**2-OCH_3**	**4-OH**	**-10.86**
CD7	2-OCH_3	4-CH_3	-9.16
CD8	**2-OCH_3**	**4-OCH_3**	**-11.32**
CD9	2-OCH_3	4-Cl	-10.22
CD10	2-OCH_3	4-F	-10.32

CD11	2-OH	4-OH	-8.11
CD12	2-OH	4-CH_3	-8.78
CD13	2-OH	4-OCH_3	-8.12
CD14	2-OH	4-Cl	-8.46
CD15	2-OH	4-F	-7.92
CD16	2-Cl	4-OH	-7.36
CD17	2-Cl	4-CH_3	-7.42
CD18	2-Cl	4-OCH_3	-7.88
CD19	**2-Cl**	**4-Cl**	**-10.92**
CD20	**2-Cl**	**4-F**	**-11.08**
CD21	2-Br	4-OH	-7.32
CD22	2-Br	4-CH_3	-7.58
CD23	2-Br	4-OCH_3	-7.12
CD24	2-Br	4-Cl	-7.16
CD25	2-Br	4-F	-7.62
CD26	2-Br	4-Br	-7.36
CD27	2-NO_2	4-OH	-9.27
CD28	**2-NO_2**	**4-CH_3**	**-11.46**
CD29	2-NO_2	4-OCH_3	-8.56
CD30	2-NO_2	4-Cl	-8.14
CD31	2-NO_2	4-F	-8.31
CD32	2-NO_2	4-Br	-9.41
CD33	2-NH_2	4-OH	-9.47
CD34	2-NH_2	4-CH_3	-8.81
CD35	2-NH_2	4-OCH_3	-8.67
CD36	2-NH_2	4-Cl	-8.08
CD37	2-NH_2	4-F	-8.18
CD38	2-NH_2	4-Br	-8.38
CD39	2-CH_3	4-OH	-8.96
CD40	2-CH_3	4-CH_3	-9.08
CD41	2-CH_3	4-OCH_3	-9.17
CD42	2-CH_3	4-Cl	-9.36
CD43	2-CH_3	4-F	-10.08
CD44	**2-CH_3**	**4-NH_2**	**-10.78**
CD45	2-F	4-OH	-9.77
CD46	2-F	4-CH_3	-9.12
CD47	2-F	4-OCH_3	-9.56
CD48	2-F	4-Cl	-9.02
CD49	2-F	4-F	-9.78
CD50	2-F	4-Br	-9.24
Exemestane			-11.28

Various interactions displayed by the best six hybrid molecules (CD6, CD8, CD19, CD20, CD28, CD44) have been displayed in Table 2 along with the distances. Various interaction poses, 2D and 3D binding patterns of these six hybrid compounds have been depicted in Figures 3 to 8 whereas binding patterns of exemestane have been depicted in Figure 9. Compounds CD8, CD20 and CD28 revealed comparable scores to exemestane with excellent interactions at very short distances. The main amino acid residue involved in interactions were CYS437, Ala306, Val370, Thr310, Met310, Pro429, Trp341, Arg435 and 411. It was evident that the best compounds revealed almost similar binding patterns as the standard drug exemestane. The main types of interactions involved in binding were hydrogen bonding, Arene-H and side chain acceptor interactions.

Table 2: Various interactions revealed by best seven designed compounds

Compound	Docking Score (PDB Id: 3S7S)	Type of Interactions & Distances
CD6	-10.86	Phe430(Arene-H interaction), Cys435(H-bond with =O; 3.95Å), Val370(H-bond with O; 2.63Å), Pro368(H-bond with O; 2.36Å), Ala306(H-bond with =O; 4.51Å)
CD8	-11.32	Ala306(Arene-H interaction), Cys437(H-bond with =O; 3.34Å), Thr310(H-bond with N; 3.17Å), Val370(H-bond with O; 2.83Å), Ala306(H-bond with -NH; 2.23Å)
CD19	-10.92	Thr310(Arene-H interaction), Cys437(Side chain acceptor interaction with H; 3.65Å), Pro429(H-bond with -NH; 2.07Å), Trp341(H-bond with Cl; 2.27Å), Arg115(H-bond with O; 3.65Å), Arg115(H-bond with =O; 3.20Å), Val370(H-bond with -NH; 4.19Å)
CD20	-11.08	Met303(Side chain acceptor interaction with H; 3.65Å),Cys437(Side chain acceptor interaction with H; 3.75Å), Cys437(Side chain acceptor interaction with H; 4.15Å), Arg435(H-bond with -NH; 2.74Å), Arg435(H-bond with =O; 3.55Å)
CD28	-11.46	Arg435(H-bond with =O; 2.08Å), Arg145(H-bond with O; 2.21Å), Pro429(H-bond with -NH; 2.14Å), Trp141(H-bond with O; 1.57Å), Val373(H-bond with –NH; 4.66Å)
CD44	-10.78	Cys437(Side chain acceptor interaction with H; 4.27Å), Cys437(H-bond with =O; 3.59Å), Ala438(Arene-H interaction), Arg155(H-bond with -NH; 3.38Å), Cys437(H-bond with -NH; 3.88Å)
Exemestane	-11.28	Met374(H bond with =O; 1.97Å), Arg115(H bond with =O; 2.63Å), Ala306(H bond with =O; 4.40Å)

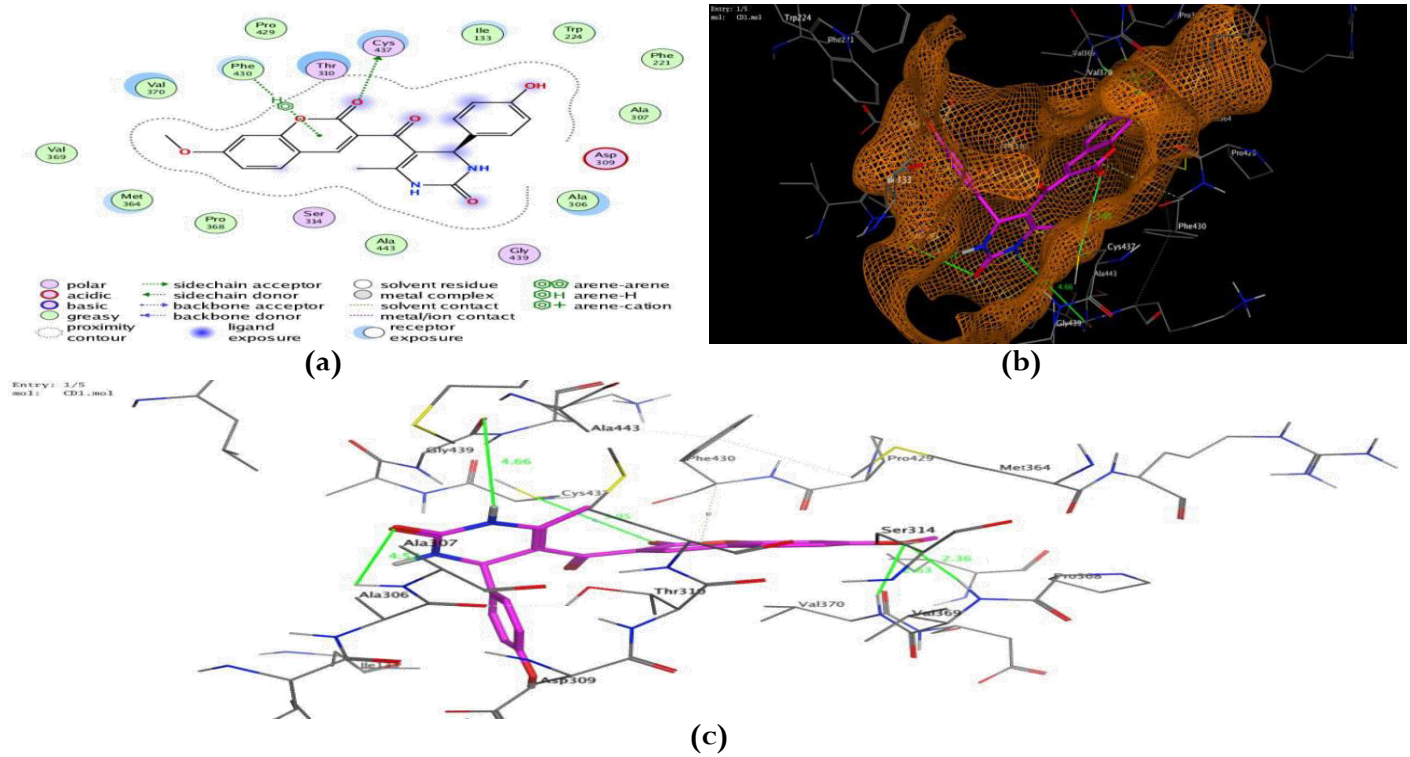

Fig. 3: Interaction poses of CD6 with aromatase (a) 2D interactions (b) CD6 embedded in receptor pocket (c) Interactions along with distances

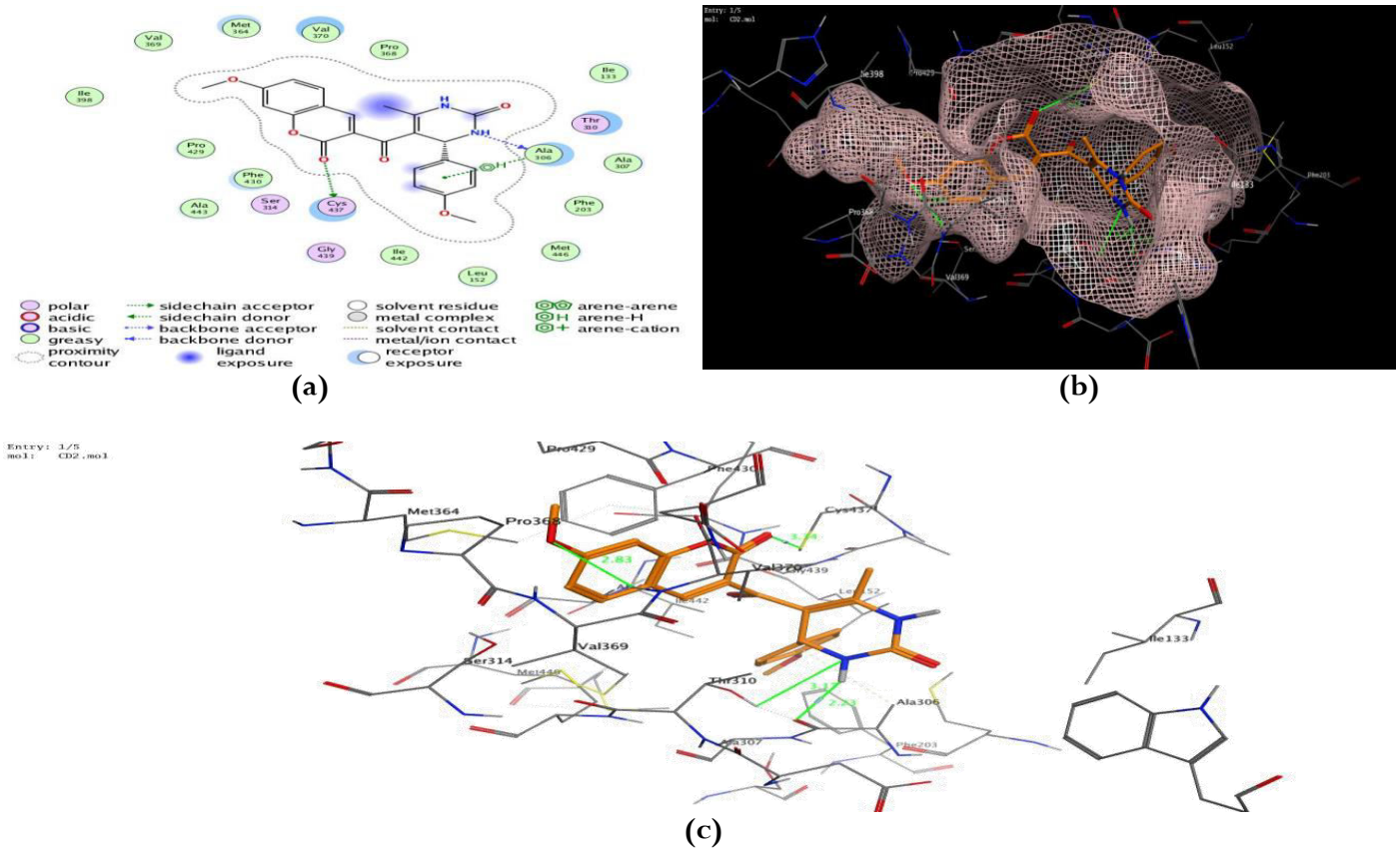

Fig. 4: Interaction poses of CD8 with aromatase (a) 2D interactions (b) CD8 embedded in receptor pocket (c) Interactions along with distances

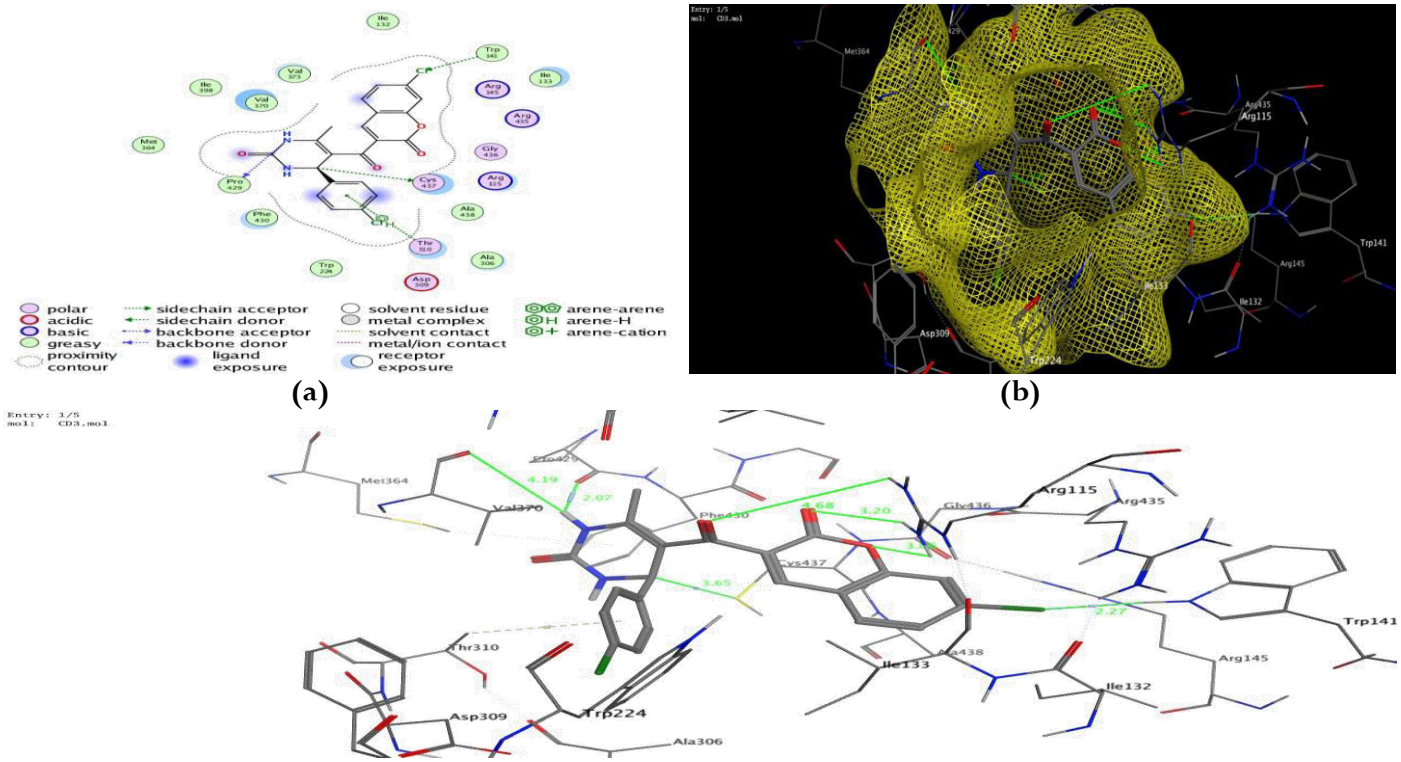

Fig. 5: Interaction poses of CD19 with aromatase (a) 2D interactions (b) CD19 embedded in receptor pocket (c) Interactions along with distances

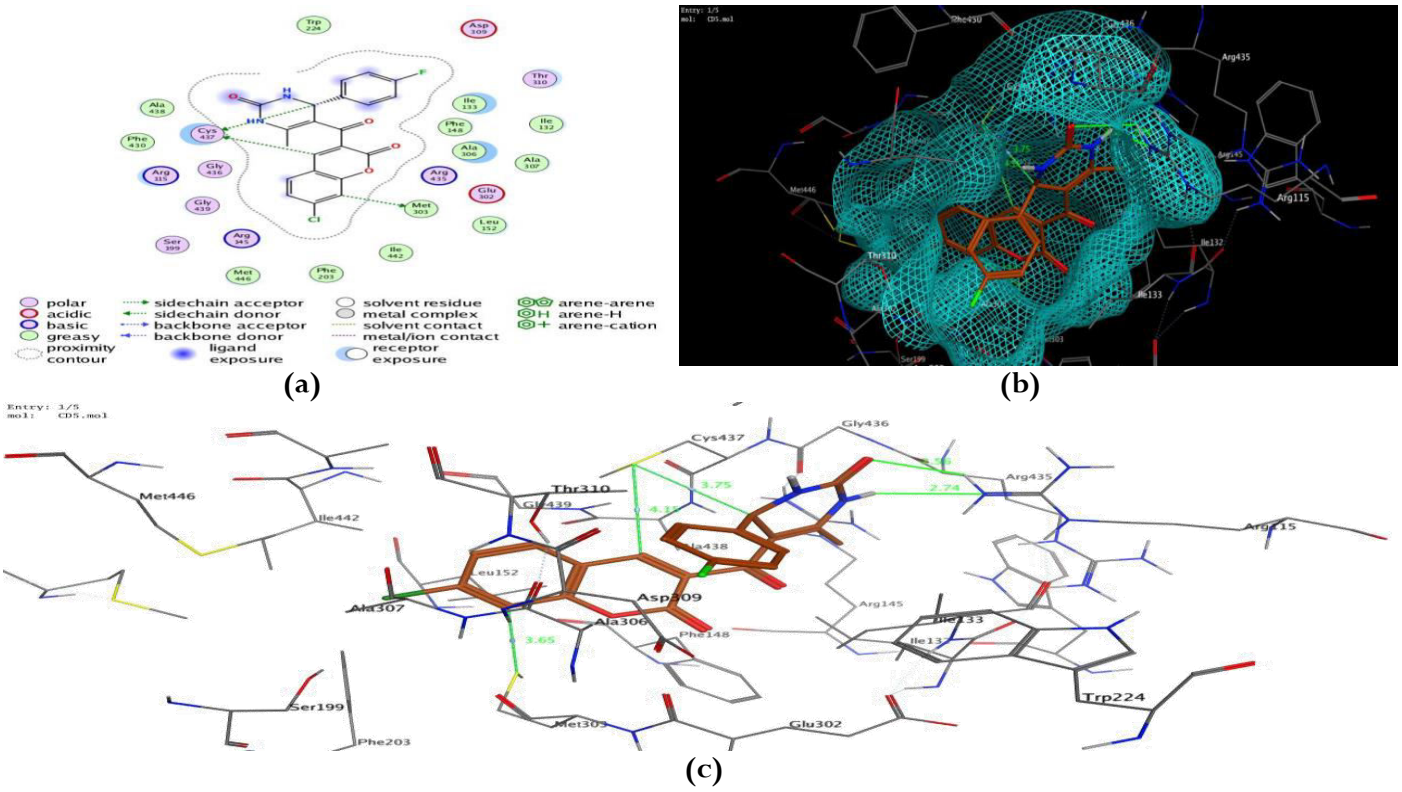

Fig. 6: Interaction poses of CD20 with aromatase (a) 2D interactions (b) CD20 embedded in receptor pocket (c) Interactions along with distances

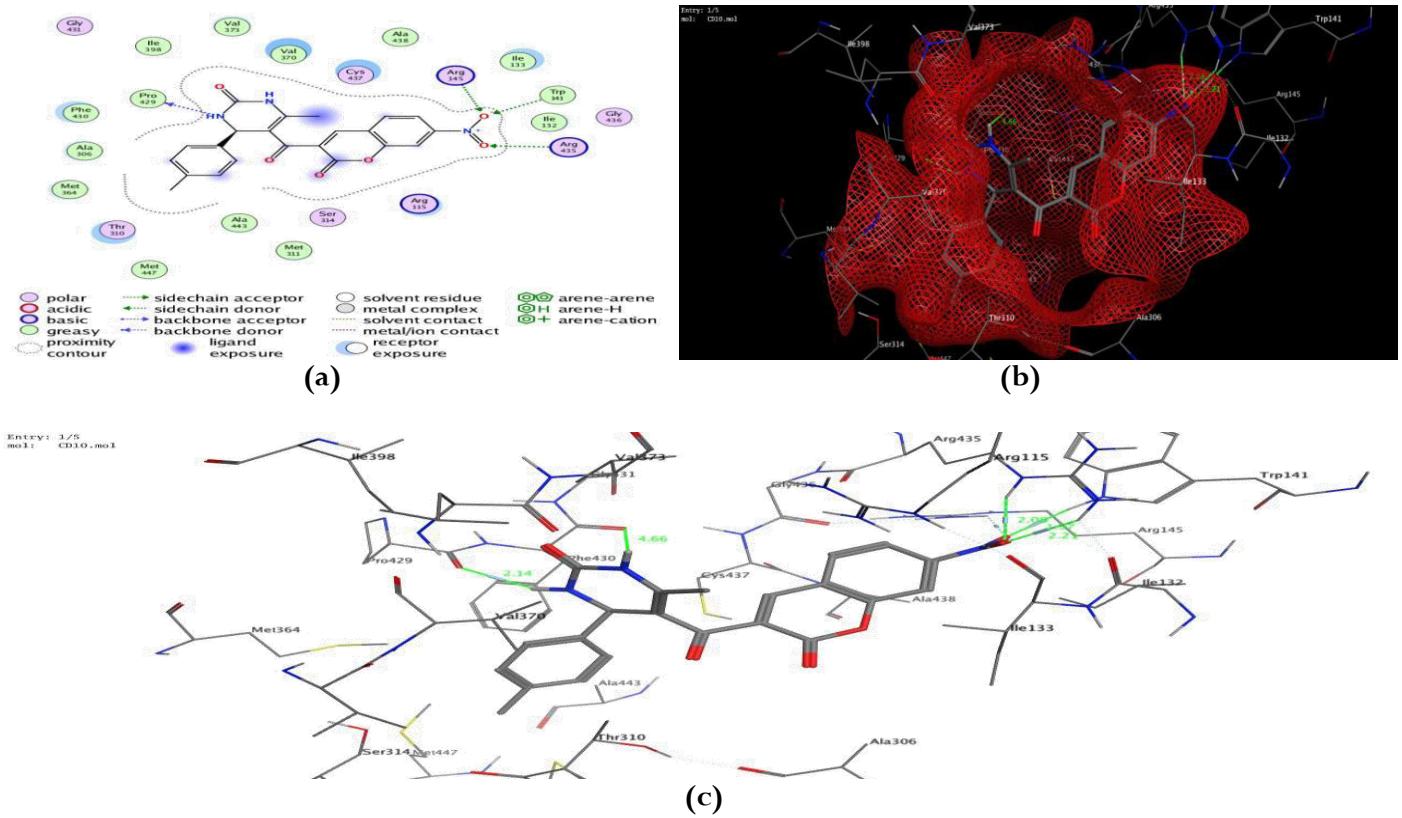

Fig. 7: Interaction poses of CD28 with aromatase (a) 2D interactions (b) CD28 embedded in receptor pocket (c) Interactions along with distances

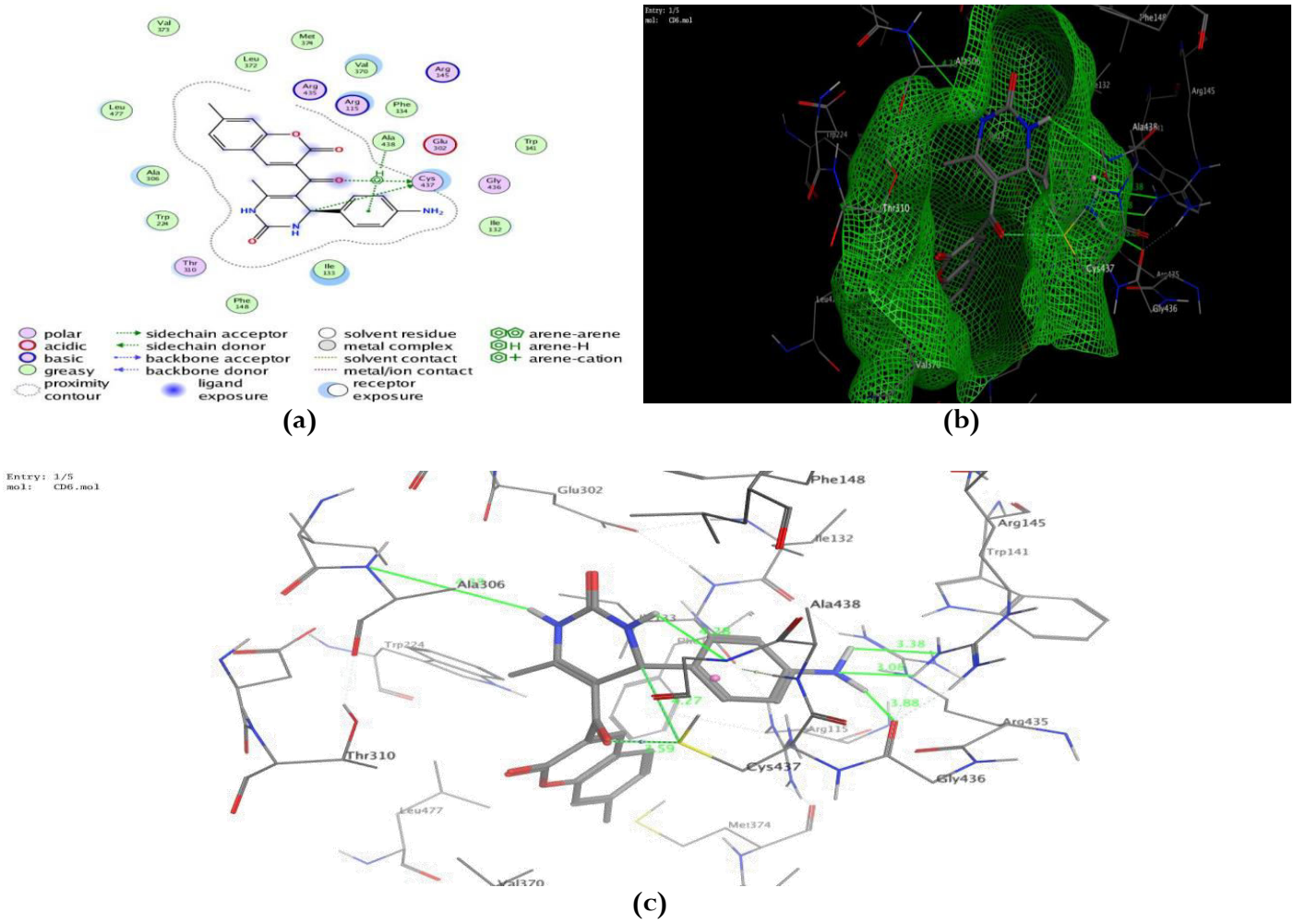

Fig. 8: Interaction poses of CD44 with aromatase (a) 2D interactions (b) CD44 embedded in receptor pocket (c) Interactions along with distances

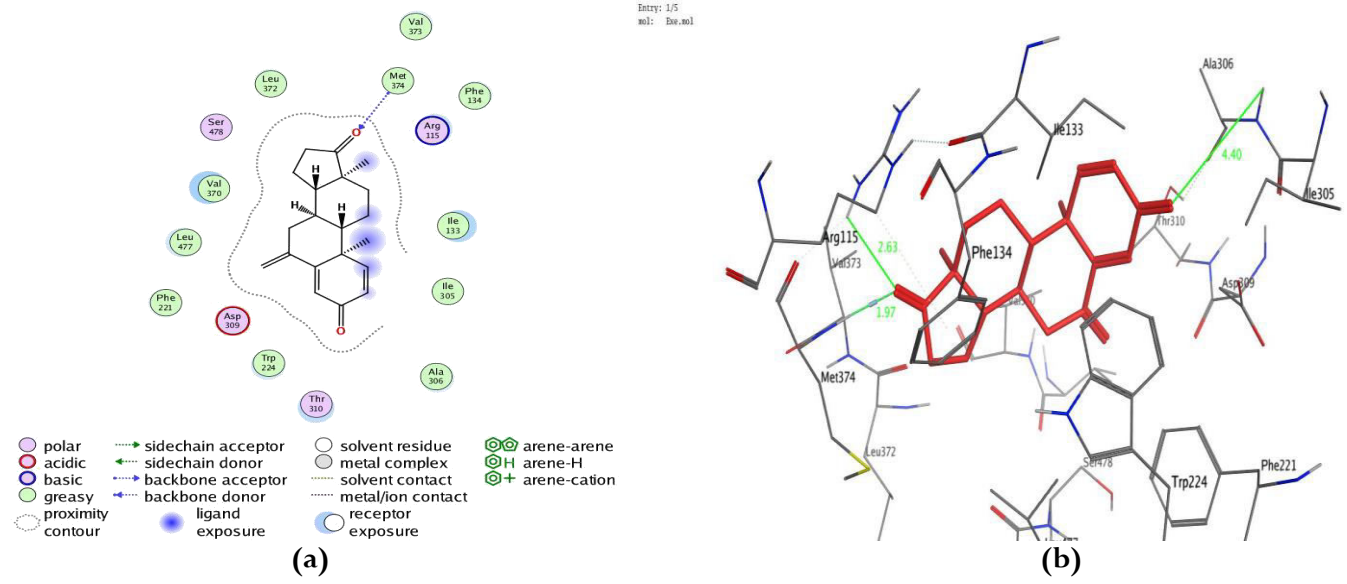

Fig. 9: Interaction poses of Exemestane with aromatase (a) 2D interactions (b) Interactions along with distances

3.2. Drug Likeliness Prediction

Drug likeliness prediction is a promising approach to get an idea about drug like properties of designed molecules. These properties are important to predict the bioavailability of drugs and medicinal chemist can modify the factors affecting it accordingly. Drug likeliness features of best six compounds were predicting by using Swiss ADME predictor. Percentage absorption (% ABS) was calculated by using formula %ABS = 109- (0.345×TPSA). The designed potent analogues displayed good absorption in the range of 76.5-82.77%. Results evidenced that designed potent analogues showed no violation of Lipinski's Rule of Five as represented in **Table 3.** Hence it can be postulated that the designed molecules may serve as drug like candidates.

Table 3: *In silico* drug like properties of best six designed hybrids

Compound	TPSA[a]	MW[b]	RoB[c]	HBD[d]	HBA[e]	IlogP (MlogP)[f]	logS[g]	% ABS[h]
Rule	**≤140**	**≤500**	**≤10**	**≤5**	**≤10**	**≤5**	**>-4**	-
CD6	117.87	406.39	4	3	6	1.30	-4.43	82.39
CD8	106.87	420.41	5	2	6	1.51	-4.53	82.39
CD19	88.41	429.25	3	2	4	3.10	-5.52	79.21
CD20	88.41	412.80	3	2	5	2.99	-4.97	76.03
CD28	134.23	419.39	4	2	6	1.47	-5.37	82.39
CD44	114.43	389.40	3	3	4	1.82	-4.42	82.39

Abbreviations:[a]Topological polar surface area; [b]Molecular weight; [c]Number of rotatable bonds; [d] Number of hydrogen bond donors; [e]Number of hydrogen bonds acceptors; [f] Logarithm of compound partition coefficient between n-octanol and water; [g]Logarithm of water solubility; [h]Percentage absorption

3.3. *In silico* Toxicty Prediction

A preliminary idea about the toxicity of a designed molecule is of utmost importance as it may be helpful to prevent the failure of it during clinical stages. The *in silico* toxicity prediction was carried out by PreADME and PROTOX softwares. Protox suggested that designed compounds lie in Class 4 with LD50 value >900 mg/kg which is much higher dose to be toxic. Carcino-Mouse and Carcino-Rat toxicity test were found positive suggesting that there is no evidence of carcinogenic toxicity. Medium risk for hERG inhibition evidenced that designed analogues have minimum risk on cardiac action potential. The predicted data have been presented in Table 4. From the data, it can be concluded that the designed molecules are safe to be used as a drug.

Table 4: *In silico* toxicity results for best six hybrid compounds

Compound	Carcino-Mouse	Carcino-Rat	HERG-inhibition	Protox Predicted LD50	Protox Predicted Class
CD6	Positive	Positive	Medium risk	1350 mg/kg	Class 4
CD8	Positive	Positive	Medium risk	1350 mg/kg	Class 4
CD19	Positive	Positive	Medium risk	1120 mg/kg	Class 4
CD20	Positive	Positive	Medium risk	1120 mg/kg	Class 4
CD28	Positive	Positive	Medium risk	1350 mg/kg	Class 4
CD44	Positive	Positive	Medium risk	1350 mg/kg	Class 4

3.4. Synthesis

The best compounds CD6, CD8, CD19, CD20, CD28 and CD44 which have been screened out after virtual screening were synthesized according to the synthetic protocol as depicted in Scheme 1.

The reaction progress was monitored by using thin layer chromatography. The physical characterization of the synthesized compounds has been depicted in Table 5. The structures of the synthesized compounds were confirmed through ^{1}HNMR, ^{13}CNMR and mass spectrometric techniques.

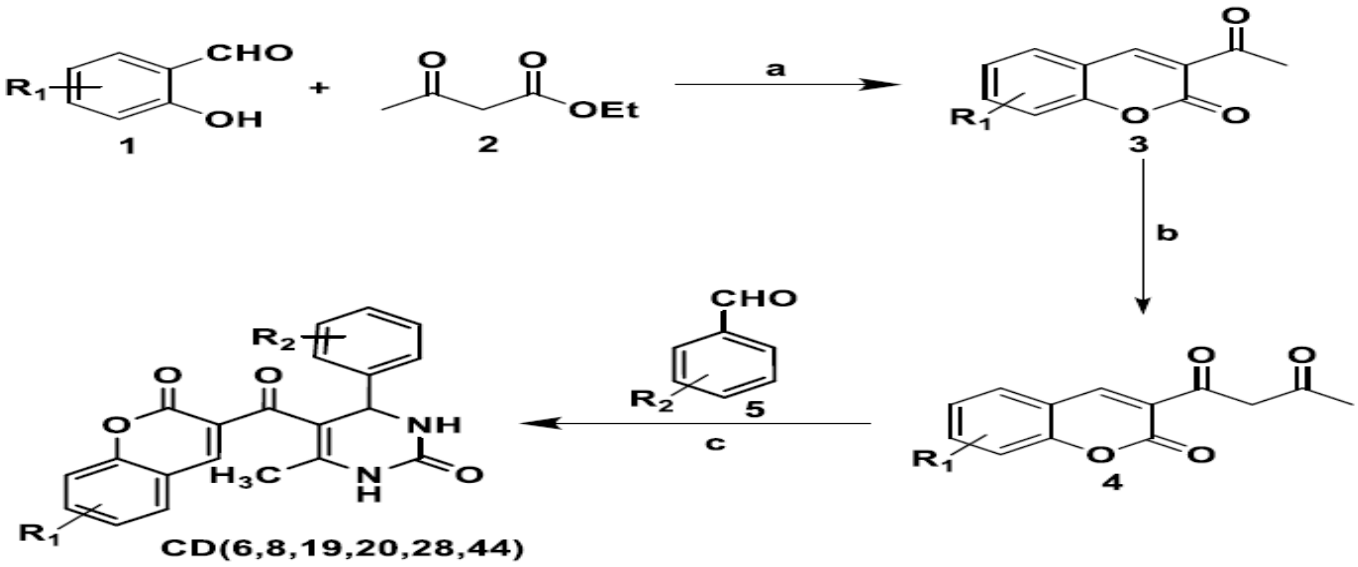

Scheme 1: (a) Piperidine, stirring for 2 hours under cold conditions (b) Potassium tertiary butoxide, ethyl acetate, stirring under cold conditions (c) Urea, acetonitrile, sulphuric acid, reflux for 4 hours

Table 5: Physical characterization of synthesized compounds

Compound	R_1	R_2	% Yield	Melting point	R_f (Hexane: Ethyl acetate)
CD6	OCH_3	OH	66	268-270 °C	0.57
CD8	OCH_3	OCH_3	72	258-261°C	0.53
CD19	Cl	Cl	56	229-233 °C	0.59
CD20	Cl	F	62	226-228 °C	0.63
CD28	NO_2	CH_3	58	245-246 °C	0.61
CD44	CH_3	NH_2	62	230-232°C	0.59

3.5. *In vitro* cytotoxic activity

The synthesized compounds were further screened out for their *in vitro* cytotoxic activity against breast cancer cell lines MCF7 and T47D. Well established colorimetric MTT assay method was utilized to determine the anti-proliferative potentials of the compounds. Marketed aromatase inhibitor exemestane was used as standard drug for comparison. The IC_{50} values in µg/mL of the compounds and standard drugs have been depicted in Table 6 and Figure 10a and 10b. All the compounds revealed good to moderate cytotoxic activity in comparison to exemestane. Compounds CD28 revealed more activity as compared to exemestane against both the cell lines whereas compound CD8 displayed almost comparable activity to exemestane. It was noteworthy here that substitution of phenyl ring attached to dihydropyrimidinone, at para position with electron donating groups displayed maximum activity. Similarly substitution of phenyl ring of coumarin at 2nd position with electron releasing groups enhanced activity whereas substitution with halogens showed moderate activity. Compound CD28 revealed exceptional structural activity relationship as it displayed maximum activity while coumarin was substituted with nitro group.

Table 6: Anticancer activity of synthesized compounds against breast cancer cell lines

Compound	IC50 (µg/mL)	
	MCF7	T47D
CD6	22.8 ± 2.18	38.82 ± 2.46
CD8	16.8 ± 0.96	22.38 ± 1.02
CD19	24.8 ± 1.12	28.2 ± 1.82
CD20	27.82 ± 1.76	32.6 ± 1.42
CD28	8.82 ± 0.26	13.82 ± 1.08
CD44	23.82 ± 1.28	26.82 ± 2.16
Exemestane	7.32 ± 0.32	18.28 ± 0.92

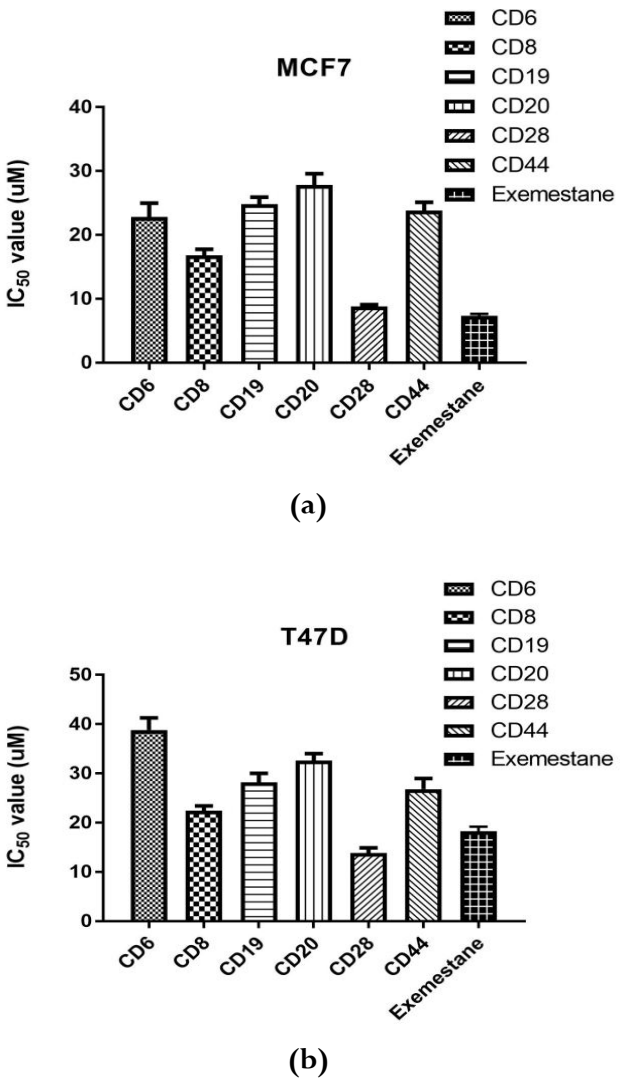

Fig. 10: Cytotoxic activity of compounds against (a) MCF7 Cell lines (b) T47D Cell lines

4. CONCLUSION

In the presented work, we have made an attempt to screen out the most potent coumarin-dihydropyrimidinone hybrids by generating a library of 50 hybrids by considering the structural features of coumarin and dihydropyrimidinone motifs. Six compounds were selected among the library on the basis of docking scores and binding patterns. These 6 were further synthesized through suitable synthetic strategy and well characterized. Further cytotoxic potential of these compounds was evaluated against breast cancer cell lines MCF7 and T47D cell lines utilizing MTT colorimetric assay. Compounds revealed good to moderate activity and compound **CD28** was found most potent among all. These compounds were also analysed for *in silico* drug like properties and showed no violation from Lipinski's Rule of 5. Also these were found least toxic through *in silico* toxicity prediction studies. Further exploration of these hybrids must be carried out by trying other substitutions and more targets should be considered for design. The reported compounds may serve as potential leads for further drug discovery and development.

5. REFERENCES

1. Zhong HA. *Curr Top Med Chem*. 2020; **20(10):**813-814.
2. Man RJ, Jeelani N, Zhou C, Yang YS. *Anticancer Agents Med Chem.*, 2020; 10.2174/1871520620666200516150345.
3. Ali I. *Current Cancer Drug Targets,* 2011; **11**:131.
4. Imran A, Mohammad NL, Al-Othman ZA, Al-Warthan A, Sanagi MM. *Current Drug Targets*, 2015; **16:**711.
5. Yaghjyan L, Colditz GA. *Cancer Causes Control*, 2011**; 22(4):**529-540.
6. Hua H, Zhang H, Kong Q *et al. Exp Hematol Oncol,* 2018; **7:**doi:/10.1186/s40164-018-0116-7.
7. Mukhopadhyay KD, Liu Z, Bandyopadhyay A, Kirma NB, Tekmal RR, Wang S *et al. PLoSONE*, 2015; **10(4):**e0121136.
8. Brueggemeier RW, Hackett JC, Diaz-Cruz ES. *Endocrine Reviews*, 2005; **26(3):**341-345.
9. Bulun SE, Price TM, Aitken J, Mahendroo MS, Simpson ER. *J Clin Endocrinol Metab*, 1993; **77:**1622-1628.
10. Bayat MR, Homayouni TS, Baluch N et al. *Oncotarget.*, 2017; **8(23):**38022-38043.
11. Sanduja M, Gupta J, Virmani T. *J Appl Pharm Sci*, 2020; **10(2):**129-146.
12. Bhatia R, Rawal RK. *Mini Rev Med Chem.*, 2019; **19(17):**1443-1458.
13. Adriano DA, Lívia BS, Donald JA. *Curr. Top. Med. Chem.*, 2009; **9(9):**771-790.
14. Mishra S, Singh P. *Eur. J. of Med. Chem.*, 2016; **124:**500-536.
15. Wang Y, Zhang W, Dong J, Gao J. *Bioorg Chem*, 2020; **95**:103530.
16. Thakur A, Singla R, Jaitak V. *Eur J Med Chem*, 2015; **101**:476-495.
17. Stefanachi A, Leonetti F, Pisani L, Catto M, Carotti A. *Molecules*, 2018; **23(2):**250.
18. José M, Marc D. *Future Medicinal Chemistry,* 2019; **11**:1057-1082.
19. Maryam MK, Fahimi K, Elahe KR, Safavi M, Mohammad M, Mina S, Tahmineh A. *Lett. Drug Design &Discov.,* 2019; **16:** 818.

20. Goud NS, Kumar P, Bharath RD. *Mini Rev Med Chem.*, 2020.
21. Kaur R, Chaudhary S, Kumar K, Gupta MK, Rawal RK. *Eur J Med Chem.*, 2017; **132**:108-134.
22. Bhat MA, Al-Dhfyan A, Al-Omar MA. *Molecules,* 2016; **21(12):**1746.
23. Amany S. Mostafa, Khalid B. Selim. *Eur J Med Chem.*, 2018; **156:**304-315.
24. Reddy OR, Suryanarayana VC, Sharmila N, Ramana GV, Anuradha V, Hari B. *Lett in Drug Design & Discov,* 2013; **10**:699.
25. Soumyanarayanan U, Bhat VG, Kar SS *et al. Org Med Chem Lett*, 2012; **2:**23.
26. Protein Data Bank. http:/www.rcsb.org/pdb
27. Lipinski CA, Lombardo F, Dominy BW, Feeney PG. *Adv. Drug Deliv. Rev.*, 2012; **64**:4-17**.**
28. Protox-II prediction of toxicity of chemicals. Available online: http://tox.charite.de/protox_II/
29. Sekhan P, Storeng R, Scudiero D et al. *J Nat Can Inst*, 1990; **82(13):**1107-1112.